

Analysis of Fibre Tip Damage Risk During Pulsed Holmium Laser Application Under Water

T. ASSHAUER, G. DELACRÉTAZ

Institut d'Optique Appliquée (IOA), Ecole Polytechnique Fédérale de Lausanne, Lausanne, Switzerland

Correspondence to G. Delacrétaz, Institut d'Optique Appliquée (IOA), École Polytechnique Fédérale de Lausanne, CH-Ecublens, CP127, CH-1015 Lausanne, Switzerland

Received 29 July 1996; accepted in final form 8 January 1997 (London)

Abstract. Breaking of optical fibre tips during medical holmium laser applications involving endoscopic irradiation in a liquid environment, such as arthroscopy, has been reported. This represents a risk of complications due to foreign body reactions induced by quartz fragments remaining at the operation site.

Fibre breakage has been analysed under controlled conditions at clinically used laser energies of 20–1000 mJ. The generation of pressure transients at the collapse of laser-induced vapour bubbles is identified as the mechanism of fibre tip destruction. Fibre damage is observed only in a confining liquid environment. The highest fibre damage occurrence is observed for laser fluences of 70–250 J cm⁻² at the bare fibre tip, at pulse durations of 200–350 µs. The fibre damage occurrence and extent increase with the fibre diameter.

Avoiding the identified dangerous fluence range or use of fibres smaller than 400 µm diameter is recommended to perform endoscopic holmium laser application with minimal fibre damage risk.

INTRODUCTION

Fibre damage has been reported during arthroscopic holmium laser application by several orthopaedists (eg 1, 2). In all reported cases, holmium laser pulses of 200–300 µs duration were delivered to the tissue in a liquid environment.

Laser-induced distal fibre tip destruction is well known in laser applications involving shorter pulse durations (1 µs or less), where mechanical effects are desired, such as lithotripsy with Q-switched Nd-YAG lasers, Alexandrite and pulsed dye lasers (3–7). In these cases, the fibre damage has been attributed to shock waves generated either during laser irradiation by plasma formation (8) or rapid thermal expansion, or at the collapse of a formed cavitation bubble (9).

Time-resolved studies of holmium laser irradiation via optical fibres into water demonstrated that transient vapour bubbles of several millimetres diameter are generated around the fibre tip (10). Recently, the present authors showed that holmium-laser-generated transient bubbles can induce, at their collapse,

shock waves with peak amplitudes in the kilobar range (11, 12), suggesting that these cavitation phenomena could be a major cause of the reported fibre damage.

In the present article, the occurrence and mechanisms of fibre tip damage during holmium laser irradiation under water are investigated. The effect of the laser pulse energy and the fibre diameter on the likelihood of damage is examined.

EXPERIMENTAL METHODS

A complete description of the experimental technique and setup developed to observe transient bubbles and record pressure transients can be found elsewhere (12). Briefly, free-running holmium laser pulses were delivered through bare 'all quartz' fibres of low OH⁻ content immersed in a de-ionized water basin. Tests were performed with fibres having core/cladding diameters of 200/240, 400/440 and 600/660 µm, respectively. In order to simulate the confined conditions encountered clinically, the fibre tip was placed at least 2 cm under

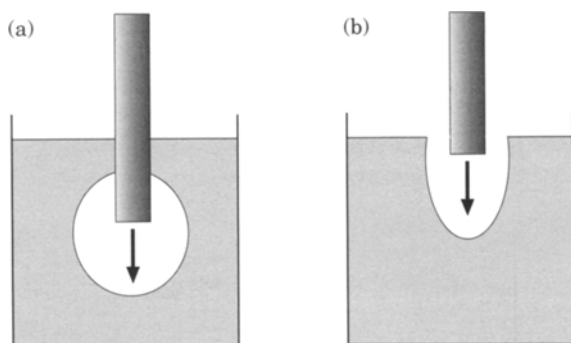


Fig. 1. Schematic of the fibre positioning and expected bubble shape. (a) Confined conditions: the fibre tip is placed 2 cm below the water surface. (b) The fibre tip is placed 0.5 mm below the water surface.

the water surface (13) [Fig. 1(a)]. In control experiments, the fibre tip was placed either in air or just 0.5 mm below the water surface [Fig. 1(b)].

A series of laser pulses with energies of 20–1000 mJ and 230 μ s in duration (full width at half maximum, FWHM), typically used in medical applications, was fired into the water at 1 Hz repetition rate. Eight different pulse energies were used for each fibre diameter. Before each experiment, the distal fibre tip was carefully cleaved and the plastic jacket was removed over a distance of 1 cm from the fibre tip. The state of the fibre tip was inspected by video microscopy (resolution 180 line pairs mm^{-1}) before and after each experiment. The experiment was repeated 10 times for each fibre diameter and laser parameter combination. The dynamics of the vapour bubbles formed around the fibre tip was observed by flash micro-videography (12), allowing observations synchronized with the laser pulses at known delay times with 1 μ s time resolution.

The correlation between fibre damage and pressure transients was studied by comparing fibre breakage occurrence and pressure amplitudes reached at the fibre tip. Pressure amplitudes at the fibre tip location were extrapolated from the amplitude measured and the pressure transducer location, assuming a pressure decrease inversely proportional to the distance to the origin of the spherical pressure wave (14) (bubble collapse centre), and taking into account the distances of the fibre tip and the pressure transducer from the collapse centre. Average peak pressures at the fibre tip were calculated from 10–15 pressure measurements per laser parameter combination, obtained in separate experiments with intact fibres.

RESULTS

Observed damage

Typical fibre damage induced during underwater holmium laser irradiation is shown in Fig. 2. The intact freshly cleaved 600 μ m fibre tip [Fig. 2(a)] was severely damaged after the delivery of 160 laser pulses [Fig. 2(b)] at a fluence of 170 J cm^{-2} (pulse energy 480 mJ). In this particular case, fibre damage started after approximately 80 pulses.

For laser fluences below 70 J cm^{-2} , no damage was observed. Increasing the laser fluence led to an increased damage occurrence. Most frequent damage occurred for laser fluences at the fibre tip ranging from 70 to 250 J cm^{-2} . Above 250 J cm^{-2} , fibre damage decreased significantly.

Tip damage was also observed for 400 μ m fibres. Maximal damage was observed at comparable laser fluences as for 600 μ m diameter fibres, ie at pulse energies 2.25 times lower than for the 600 μ m fibres. However, fibre damage occurred only after larger numbers of pulses and was less significant. Cracks were observed at the tip, but no large splinters. In general, at least 200 pulses were required to induce significant damage.

For the smallest fibres studied, with 200 μ m core diameter, no damage was observed over the whole range of pulse energies investigated, ie for laser fluences up to 3 kJ cm^{-2} .

When pulses were fired in air, no damage could be detected, even at the highest tested pulse energy of 1 J and for more than 1000 pulses. Also, when the fibre tip was placed slightly below the water surface, no damage could be observed.

Time-resolved observation of damage progression

The on-line recording of damage progression was obtained by time-resolved flash videography. An example of fibre damage onset and progression can be seen in Fig. 3.

In the case shown, laser pulses of 230 μ s duration and an energy of 480 mJ were delivered via a 600 μ m core diameter fibre (170 J cm^{-2} at the fibre tip). After 50 pulses, the fibre was still intact [Fig. 3(a)]. A first crack was observed after 82 pulses [Fig. 3(b), arrow], resulting in a splitting of the fibre tip at the 91st pulse [Fig. 3(c), arrow]. The rebound

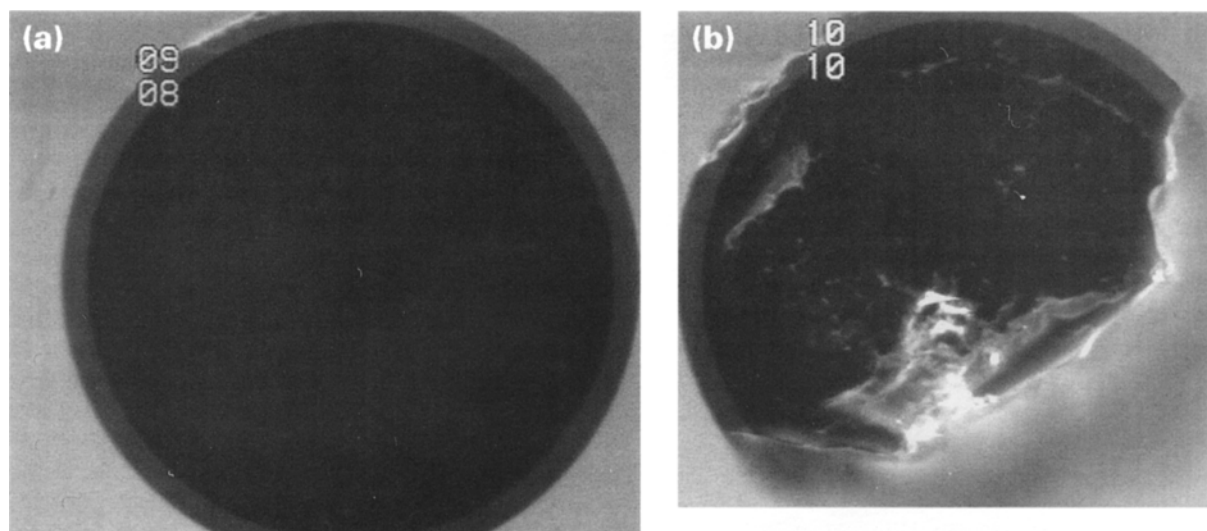


Fig. 2. (a) Cleaved fibre tip before experiment: core diameter $600\text{ }\mu\text{m}$, cladding $30\text{ }\mu\text{m}$. (b) Fibre tip state after 160 laser pulses of 170 J cm^{-2} and $230\text{ }\mu\text{s}$ duration (full width at half maximum) fired under water.

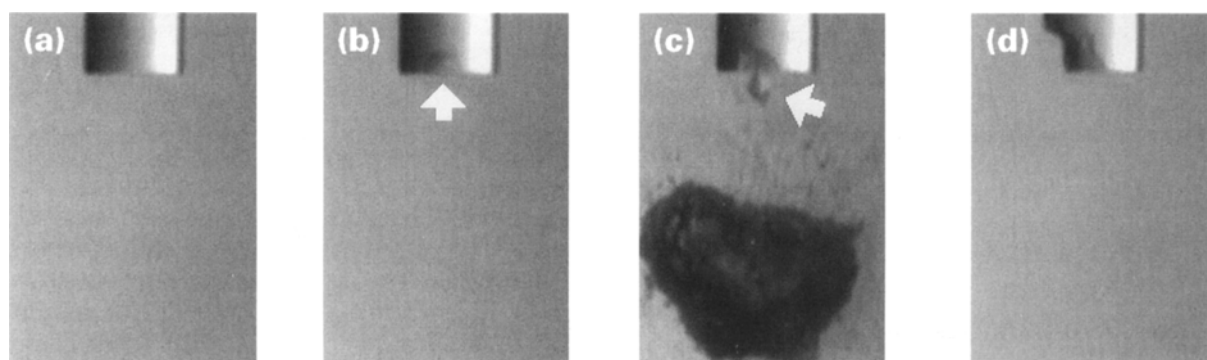


Fig. 3. Example of fibre tip degradation after increasing numbers of laser pulses (170 J cm^{-2} , $230\text{ }\mu\text{s}$ duration) under water, fibre diameter $600\text{ }\mu\text{m}$. (a) After 50 pulses, (b) after 82 pulses, (c) after 91 pulses, image taken $50\text{ }\mu\text{s}$ after bubble collapse, (d) after 150 pulses.

(re-expansion phase) of the cavitation bubble formed can be seen in Fig. 3(c) (see below for complete description of the cavitation process). Subsequent laser pulses continued to damage the fibre and split further fragments off the tip until the final result shown in Fig. 3(d). Fragment ejection was only observed at the bubble collapse. The fragments were projected up to 4 mm away from the fibre within some milliseconds after the bubble collapse due to the liquid flow induced by the bubble dynamics.

Dynamics of bubbles formed in deep water or near the surface

The dynamics of bubbles formed near the surface and in deep water have been compared. When the fibre tip was deeply immersed in

water, a transient vapour bubble was created around the fibre tip for each laser pulse above the threshold fluence of $25 \pm 5\text{ J cm}^{-2}$, generating shock waves at its collapse. The bubble, containing water vapour, was formed, expanded and collapsed on a typical time scale of less than 1 ms . Such a transient bubble is shown in Fig. 4(a). At its collapse, after a lifetime of $700\text{ }\mu\text{s}$ [Fig. 4(b)], a pressure transient was generated, as reported previously (12). Some milliseconds after the laser pulse, the bubble had completely vanished by condensation of its vapour contents.

By comparison, the dynamics of bubbles formed near the surface was different. Figure 5 shows the behaviour of a bubble formed at the tip of a $600\text{ }\mu\text{m}$ core diameter fibre placed 0.5 mm below the surface. During laser irradiation (radiant exposure 170 J cm^{-2} , pulse duration $230\text{ }\mu\text{s}$ FWHM), a transient channel, open

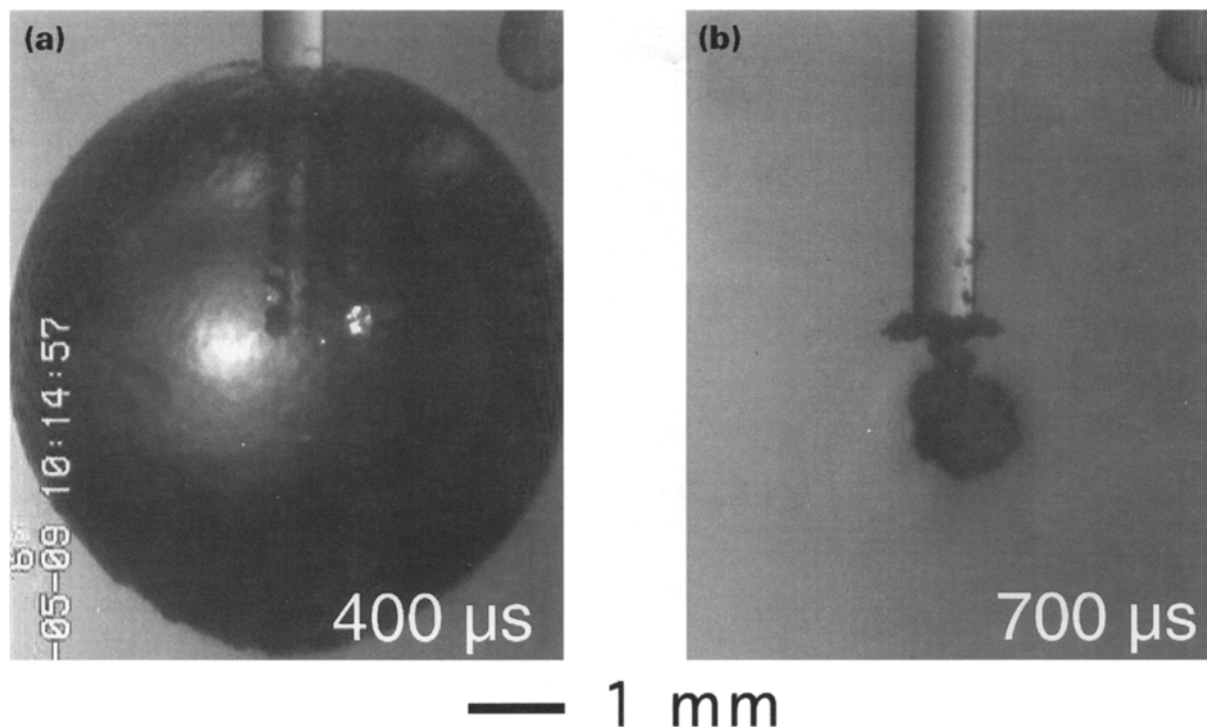


Fig. 4. Bubble generated at the tip of an immersed fibre ($600\text{ }\mu\text{m}$ core diameter, radiant exposure 170 J cm^{-2} , pulse duration $230\text{ }\mu\text{s}$ full width at half maximum). The tip of a pressure transducer is visible in the right upper image corner.

to the free surface, was formed [Fig. 5(b)] and filled up with air sucked in from the surface. In the cooling stage after the end of the laser pulse, the water vapour condensed until a bubble filled with non-condensable air remained. As a consequence, the bubble did not completely collapse, but performed irregular oscillations for a duration of 80–100 ms [Fig. 5(c–e)]. During this time, the bubble was drawn down several millimetres below the water surface [Fig. 5(d)], due to the flow induced in the liquid. It finally rose slowly back to the surface as a permanent gas bubble by its buoyancy [Fig. 5(e)]. In the present experiment, no shock waves were detected.

Correlation of observed damage and measured pressure transients

The correlation between fibre damage and pressure transients has been studied by comparing fibre breakage occurrence and pressure amplitude data. The average peak pressures at the fibre tip position, calculated from 10–15 pressure measurements per laser parameter combination (energy and fibre diameter), and the damage occurrence are listed in Table 1.

A good correlation between the peak pressure generated and the risk of fibre damage can be seen. In particular, the fluence range for maximum fibre damage correlates with the range for maximum pressure transient generation (see Table 1). In Fig. 6, the observed peak pressures are plotted as a function of pulse energy. As no fibre damage was observed for the $200\text{ }\mu\text{m}$ fibre, only the pulse energy generating maximum pressure is shown. At higher laser energy, a decrease of the maximal pressure was observed, as for the two other fibre diameters. It can clearly be seen that the same pulse energy induces very different peak pressures depending on the fibre diameter used.

DISCUSSION

Damage was induced in the present experiments only when the fibre tip was placed deep below the water surface. The absence of damage when laser pulses were delivered in air confirms the important role of the water environment for the fragmentation mechanism. The damage is not due to a direct interaction of the laser radiation with the fibre material, as observed for short pulse ($<10\text{ }\mu\text{s}$)

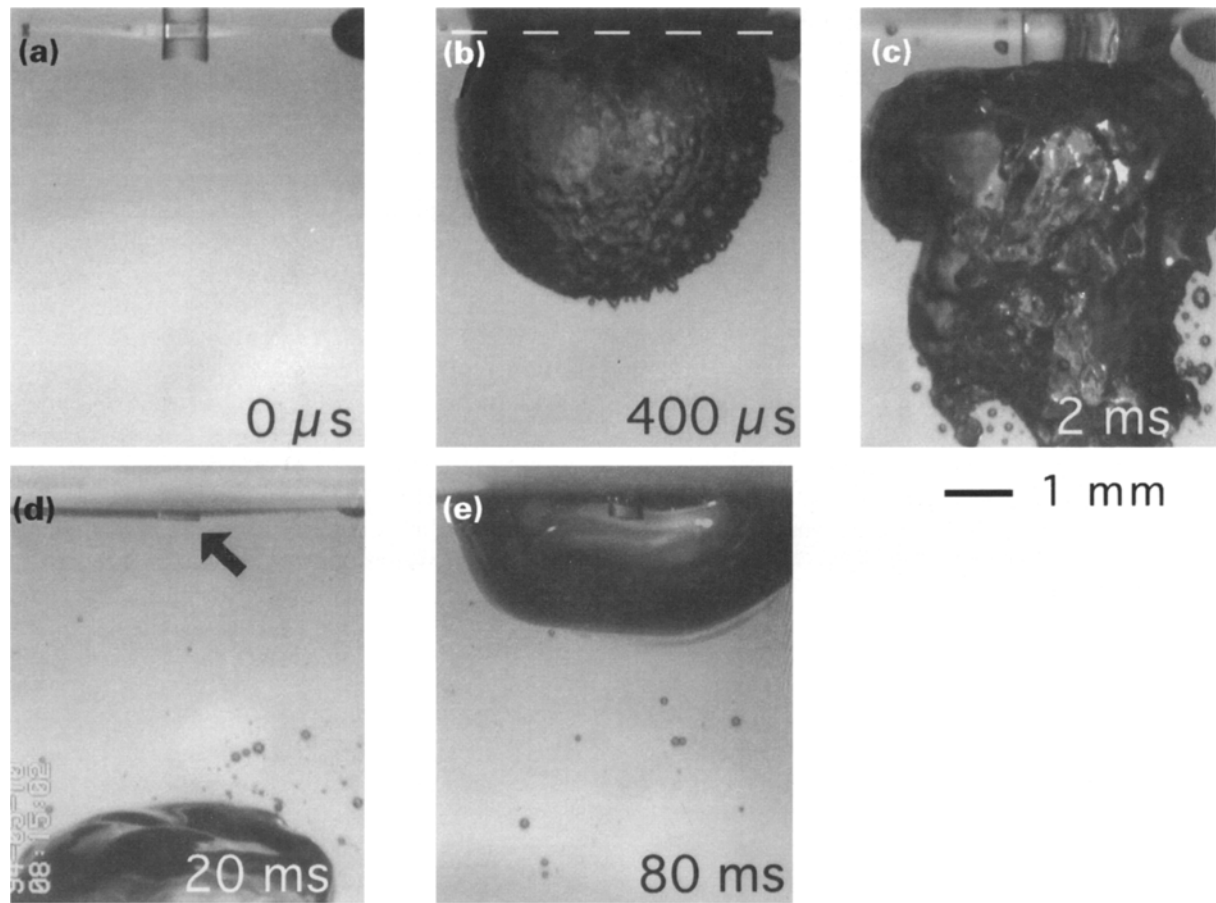


Fig. 5. Bubble dynamics at fibre tip 0.5 mm below water surface (600 μm core diameter, radiant exposure 170 J cm^{-2} , pulse duration 230 μs full width at half maximum). The white broken line indicates the initial water surface position.

Table 1. Correlation of peak pressure at the fibre tip, laser energy, laser fluence and fibre surface damage for different fibre diameters

Fibre core diameter (μm)	Pulse energy (mJ)	Fluence at fibre tip (J cm^{-2})	Average peak pressure at fibre tip (bar)	Damage occurrence
200	53	170	236	No
400	65	52	462	No
400	150	120	632	Yes
400	212	160	507	Yes
400	417	332	202	No
600	131	46	244	No
600	244	86	574	Yes
600	480	170	723	Yes
600	690	244	538	Yes
600	890	315	372	No

lasers that produce sufficiently high peak irradiances ($>10^8 \text{ W cm}^{-2}$) to create optical damage at the fibre tip at relatively low pulse energies of 10–100 mJ (7, 15). Indeed, the highest peak irradiances of the holmium laser pulses investigated in the present study (pulse

energies up to 1.0 J delivered via 200 μm diameter fibres) were at least an order of magnitude lower ($<10^7 \text{ W cm}^{-2}$). As no damage was observed when the fibre was placed slightly below the surface, an effect due to the mere contact of water with the fibre, such as a

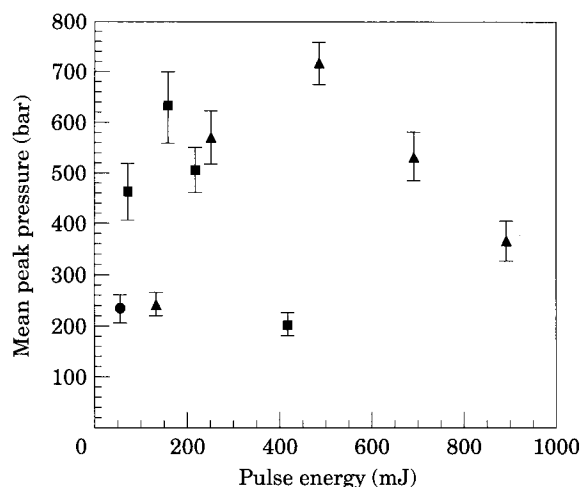


Fig. 6. Mean peak pressure at the fibre tip position as a function of laser energy for bare fibres of 200 (●), 400 (■) and 600 (▲) μm diameter. The error bars represent the standard error.

lowering of the optical damage threshold of the fibre, can be ruled out.

Thus the confinement of the laser energy and the ablation products by the surrounding water is crucial for fibre damage. The hypothesis of shock-wave generation at the bubble collapse as the damage mechanism is consistent with all experimental evidence collected. The laser fluences of 120–200 J cm^{-2} inducing the strongest fibre tip damage coincide exactly with those generating the strongest shock waves according to the authors' previous study (12).

The present pressure amplitude analysis (Table 1) suggests that the pressure threshold for damaging the fibre lies around 500 ± 100 bars at the fibre tip position. For pressures above this threshold, several pressure transients are required to induce visible damage, as typical of stress-induced material fatigue processes (16). At higher pressure amplitudes, a lower number of shocks is sufficient to induce fragmentation. Pressures generated with 200 μm diameter fibres at all the laser energies studied lie below the danger limit of fibre breakage.

The reported pressure threshold is related to the specific mechanism of bubble formation by some hundred microseconds duration holmium laser pulses. Results on fibre damage obtained with other lasers suggest that in addition to the pressure amplitude, the rise time of the pressure pulses also plays a significant role (3). This has to be taken into account when comparing the above pressure damage threshold with those reported for shock waves generated

by lasers of shorter pulse duration and higher peak power.

An additional important result of the present study is the observation of a fluence window of maximal damage occurrence for fibre diameters above or equal to 400 μm . If no critical zone has been seen for fibre diameters of 200 μm , frequent fibre damage is observed at larger fibre diameters in a specific range of fluences, in which the highest peak pressures are also generated at the bubble collapse. This range is between 70 and 250 J cm^{-2} for the 600 μm fibres and 100–200 J cm^{-2} for the 400 μm fibres. For 600 μm fibres, this corresponds to pulse energies of 200–700 mJ. Energies in this range are used during current clinical holmium laser arthroscopic procedures. For higher fluences, a reduction of the maximal pressure is observed and fibre damage is no longer induced. This effect is again related to the characteristics of the bubble dynamics generated by free-running holmium lasers of several hundred microseconds pulse duration. Due to the interaction between the expanding cavitation bubble and the ongoing laser radiation, elongated non-spherical bubbles are formed. The degree of asymmetry of the bubbles is correlated to the laser fluence, with increasingly elongated shapes for increasing fluences. The collapse of such bubbles is then much more complex, with multiple collapse centres, thus considerably reducing the strength of the induced acousto-mechanical activity (12, 17).

Control of fibre fracture risk during holmium laser clinical use is of great relevance. Indeed, the breaking of the delivery fibre during clinical use of holmium lasers could be a limiting factor for routine use in hospitals. Two major deleterious effects have to be considered. Firstly, quartz splinters remaining in the treated organ after laser treatment can cause further tissue damage and complications (5, 7). In a recent animal model study of holmium laser treatment of osteoarthritis, inflammation and foreign body reactions observed during the wound healing of knee joints were attributed to quartz fibre splinters (1). Secondly, a damaged fibre tip alters the delivered laser beam profile, thus preventing a precise dosimetry of the applied laser energy.

The present data have shown that damage risks can be minimized by choosing appropriate delivery systems. Small diameter fibres reduce the strength of the generated transients, thus reducing fibre fragmentation risks.

Another possible approach to reduce pressure transient generation and thus fibre tip fragmentation is the use of longer pulse durations than in the present study at identical laser fluence (17, 18). However, pulse duration cannot be chosen in most currently available medical holmium laser systems.

CONCLUSIONS

Breaking of delivery fibre tips in operating conditions used during endoscopic holmium laser applications in a liquid environment has been confirmed. This implies the risk of quartz fragments at the operation site.

A direct correlation was found between the maximal pressure generated at the collapse of laser-induced vapour bubbles and the occurrence and extent of fibre tip damage. For standard medical holmium laser pulse durations of 200–350 μs , the strongest damage is induced on bare fibres of more than 400 μm diameter in combination with laser fluences at the fibre tip of 70–250 J cm^{-2} . Avoiding this fluence range or use of smaller fibres minimizes the risk of fibre damage. Medical laser delivery systems and laser parameters can be optimized according to these results.

ACKNOWLEDGEMENTS

The authors would like to thank K. Rink for reading the manuscript and helpful discussions, and R.P. Salathé for his support. The support of this work by the Swiss priority programme 'Optical Sciences, Applications and Technologies' is gratefully acknowledged.

REFERENCES

- 1 Möller KO, Lind BM, Karcher K, Hohlbach G. Holmium Laser versus mechanische Knorpelabtragung. Vergleichende Untersuchung am Arthrosemodell bei Kaninchen. *Langenbecks Arch Chir* 1994, **379**:84–94
- 2 Dorn U. *Laserarthroskopie am Kniegelenk des Deutschen Landschweins*. MD Thesis (Dr. der Veterinärmedizin). Freie Universität Berlin, 1994 (unpubl.)
- 3 Rink K, Delacrétaz G, Salathé RP. Fragmentation process of current laser lithotriptors. *Lasers Surg Med* 1995, **16**:134–46

- 4 Thomas S, Pensel J, Engelhardt R, Meyer W, Hofstetter A. The pulsed dye laser versus Q-switched Nd:YAG laser in laser induced shockwave lithotripsy. *Lasers Surg Med* 1988, **8**: 363–70
- 5 Bruhn EW, Go P, McClane RW, Hunter JG, Straight RC. Biological consequences of fiber fragmentation with pulsed laser lithotripsy. In: *Laser Surgery: Advanced Characterization, Therapeutics, and Systems II*. Los Angeles, 1990. *Proc. SPIE* **1200**:90–3
- 6 Brinkmann R, Meyer W, Engelhardt R, Walling JC. Laser induced shockwave lithotripsy by use of an 1 μs Alexandrite laser. In: *Laser Surgery: Advanced Characterization, Therapeutics, and Systems II*. Los Angeles, 1990. *Proc. SPIE* **1200**:67–74
- 7 Strunge C, Brinkmann R, Flemming G, Engelhardt R. Interspersion of fragmented fiber's splinters into tissue during pulsed alexandrite laser lithotripsy. *Lasers Surg Med* 1991, **11**:183–7
- 8 Rink K, Delacrétaz G, Salathé RP. Fragmentation process induced by nanosecond laser pulses. *Appl Phys Lett* 1992, **61**:2644–6
- 9 Rink K, Delacrétaz G, Salathé RP. Fragmentation process induced by microsecond laser pulses during lithotripsy. *Appl Phys Lett* 1992, **61**:258–60
- 10 van Leeuwen TG, van der Veen MJ, Verdaasdonk RM, Borst C. Noncontact tissue ablation by holmium:YSGG laser pulses in blood. *Lasers Surg Med* 1991, **11**:26–34
- 11 Asshauer T, Rink K, Delacrétaz GP et al. Acoustic transient generation in pulsed holmium laser ablation underwater. In: *Laser-Tissue Interaction V*. Los Angeles, 1994. *Proc. SPIE* **213A**:423–33
- 12 Asshauer T, Rink K, Delacrétaz G. Acoustic transient generation by holmium laser induced cavitation bubbles. *J Appl Phys* 1994, **76**:5007–13
- 13 Blake JR, Taib BB, Doherty G. Transient cavities near boundaries. Part 2. Free surface. *J Fluid Mech* 1987, **181**:197–212
- 14 Plesset MS. Shock waves from cavity collapse. *Philos Trans Roy Soc London A* 1966, **260**: 241–4
- 15 Tschepe J, Gundlach P, Hopf J, Leege N, Müller G, Scherer H. Faserabbrand beim Alexandrit-Laser: ein Problem der laserinduzierten Stosswellen Lithotripsie. *Lasermedizin* 1991, **7**: 162–6
- 16 Brennen CE. *Cavitation and Bubble Dynamics*. Oxford: Oxford University Press, 1995 (Oxford Engineering Series 44)
- 17 Asshauer T, Jansen ED, Frenz M, Delacrétaz G, Welch AJ. Acoustic transients in pulsed holmium laser ablation: Effects of pulse duration. In: *Laser Interaction with Hard and Soft Tissue II*. Lille, 1994. *Proc. SPIE* **2323**:117–29
- 18 Jansen ED, Asshauer T, Frenz M, Motamedi M, Delacrétaz G, Welch AJ. Effect of pulse duration on bubble formation and laser-induced pressure waves during holmium laser ablation. *Lasers Surg Med* 1996, **18**:278–93

Key words: Holmium laser; Ablation; Arthroscopy; Cavitation; Vapour bubbles; Pressure transients